CLEO CONF 98-12
ICHEP98 856

Measurement of the $\bar{B} \to D\ell\bar{\nu}$ branching fractions and Form Factor Parameters

CLEO Collaboration

(July 21, 1998)

Abstract

We have studied $\bar{B} \to D\ell\bar{\nu}$ decay, where ℓ can be either e or μ. We reconstruct D and lepton pairs and distinguish $B \to D\ell\bar{\nu}$ from other B semileptonic decays by examining the net momentum and energy of the particles recoiling against the $D-\ell$ pair. We find $\Gamma(B \to D\ell\bar{\nu}) = (14.4 \pm 1.2 \pm 1.1 \pm 0.8) ns^{-1}$ and derive the branching fractions for $B^- \to D^0\ell\bar{\nu}$ and $\bar{B^0} \to D^+\ell\bar{\nu}$ of $(2.33 \pm 0.19 \pm 0.19 \pm 0.14)\%$ and $(2.25 \pm 0.19 \pm 0.18 \pm 0.13)\%$, respectively, where the uncertainties are statistical, systematic, and due to uncertainty in D decay branching fractions and the B lifetime . We also investigate the form factor and the implication of the result for $|V_{cb}|$.

M. Artuso,[1] E. Dambasuren,[1] S. Kopp,[1] G. C. Moneti,[1] R. Mountain,[1] S. Schuh,[1] T. Skwarnicki,[1] S. Stone,[1] A. Titov,[1] G. Viehhauser,[1] J.C. Wang,[1] J. Bartelt,[2] S. E. Csorna,[2] K. W. McLean,[2] S. Marka,[2] Z. Xu,[2] R. Godang,[3] K. Kinoshita,[3] I. C. Lai,[3] P. Pomianowski,[3] S. Schrenk,[3] G. Bonvicini,[4] D. Cinabro,[4] R. Greene,[4] L. P. Perera,[4] G. J. Zhou,[4] S. Chan,[5] G. Eigen,[5] E. Lipeles,[5] J. S. Miller,[5] M. Schmidtler,[5] A. Shapiro,[5] W. M. Sun,[5] J. Urheim,[5] A. J. Weinstein,[5] F. Würthwein,[5] D. E. Jaffe,[6] G. Masek,[6] H. P. Paar,[6] E. M. Potter,[6] S. Prell,[6] V. Sharma,[6] D. M. Asner,[7] J. Gronberg,[7] T. S. Hill,[7] D. J. Lange,[7] R. J. Morrison,[7] T. K. Nelson,[7] D. Roberts,[7] B. H. Behrens,[8] W. T. Ford,[8] A. Gritsan,[8] H. Krieg,[8] J. Roy,[8] J. G. Smith,[8] J. P. Alexander,[9] R. Baker,[9] C. Bebek,[9] B. E. Berger,[9] K. Berkelman,[9] V. Boisvert,[9] D. G. Cassel,[9] D. S. Crowcroft,[9] M. Dickson,[9] S. von Dombrowski,[9] P. S. Drell,[9] K. M. Ecklund,[9] R. Ehrlich,[9] A. D. Foland,[9] P. Gaidarev,[9] R. S. Galik,[9] L. Gibbons,[9] B. Gittelman,[9] S. W. Gray,[9] D. L. Hartill,[9] B. K. Heltsley,[9] P. I. Hopman,[9] J. Kandaswamy,[9] D. L. Kreinick,[9] T. Lee,[9] Y. Liu,[9] N. B. Mistry,[9] C. R. Ng,[9] E. Nordberg,[9] M. Ogg,[9,*] J. R. Patterson,[9] D. Peterson,[9] D. Riley,[9] A. Soffer,[9] B. Valant-Spaight,[9] A. Warburton,[9] C. Ward,[9] M. Athanas,[10] P. Avery,[10] C. D. Jones,[10] M. Lohner,[10] C. Prescott,[10] A. I. Rubiera,[10] J. Yelton,[10] J. Zheng,[10] G. Brandenburg,[11] R. A. Briere,[11] A. Ershov,[11] Y. S. Gao,[11] D. Y.-J. Kim,[11] R. Wilson,[11] H. Yamamoto,[11] T. E. Browder,[12] Y. Li,[12] J. L. Rodriguez,[12] S. K. Sahu,[12] T. Bergfeld,[13] B. I. Eisenstein,[13] J. Ernst,[13] G. E. Gladding,[13] G. D. Gollin,[13] R. M. Hans,[13] E. Johnson,[13] I. Karliner,[13] M. A. Marsh,[13] M. Palmer,[13] M. Selen,[13] J. J. Thaler,[13] K. W. Edwards,[14] A. Bellerive,[15] R. Janicek,[15] P. M. Patel,[15] A. J. Sadoff,[16] R. Ammar,[17] P. Baringer,[17] A. Bean,[17] D. Besson,[17] D. Coppage,[17] C. Darling,[17] R. Davis,[17] S. Kotov,[17] I. Kravchenko,[17] N. Kwak,[17] L. Zhou,[17] S. Anderson,[18] Y. Kubota,[18] S. J. Lee,[18] R. Mahapatra,[18] J. J. O'Neill,[18] R. Poling,[18] T. Riehle,[18] A. Smith,[18] M. S. Alam,[19] S. B. Athar,[19] Z. Ling,[19] A. H. Mahmood,[19] S. Timm,[19] F. Wappler,[19] A. Anastassov,[20] J. E. Duboscq,[20] K. K. Gan,[20] T. Hart,[20] K. Honscheid,[20] H. Kagan,[20] R. Kass,[20] J. Lee,[20] H. Schwarthoff,[20] A. Wolf,[20] M. M. Zoeller,[20] S. J. Richichi,[21] H. Severini,[21] P. Skubic,[21] A. Undrus,[21] M. Bishai,[22] S. Chen,[22] J. Fast,[22] J. W. Hinson,[22] N. Menon,[22] D. H. Miller,[22] E. I. Shibata,[22] I. P. J. Shipsey,[22] S. Glenn,[23] Y. Kwon,[23,†] A.L. Lyon,[23] S. Roberts,[23] E. H. Thorndike,[23] C. P. Jessop,[24] K. Lingel,[24] H. Marsiske,[24] M. L. Perl,[24] V. Savinov,[24] D. Ugolini,[24] X. Zhou,[24] T. E. Coan,[25] V. Fadeyev,[25] I. Korolkov,[25] Y. Maravin,[25] I. Narsky,[25] R. Stroynowski,[25] J. Ye,[25] and T. Wlodek[25]

[1]Syracuse University, Syracuse, New York 13244
[2]Vanderbilt University, Nashville, Tennessee 37235
[3]Virginia Polytechnic Institute and State University, Blacksburg, Virginia 24061
[4]Wayne State University, Detroit, Michigan 48202
[5]California Institute of Technology, Pasadena, California 91125
[6]University of California, San Diego, La Jolla, California 92093
[7]University of California, Santa Barbara, California 93106

[*]Permanent address: University of Texas, Austin TX 78712.

[†]Permanent address: Yonsei University, Seoul 120-749, Korea.

[8]University of Colorado, Boulder, Colorado 80309-0390
[9]Cornell University, Ithaca, New York 14853
[10]University of Florida, Gainesville, Florida 32611
[11]Harvard University, Cambridge, Massachusetts 02138
[12]University of Hawaii at Manoa, Honolulu, Hawaii 96822
[13]University of Illinois, Urbana-Champaign, Illinois 61801
[14]Carleton University, Ottawa, Ontario, Canada K1S 5B6
and the Institute of Particle Physics, Canada
[15]McGill University, Montréal, Québec, Canada H3A 2T8
and the Institute of Particle Physics, Canada
[16]Ithaca College, Ithaca, New York 14850
[17]University of Kansas, Lawrence, Kansas 66045
[18]University of Minnesota, Minneapolis, Minnesota 55455
[19]State University of New York at Albany, Albany, New York 12222
[20]Ohio State University, Columbus, Ohio 43210
[21]University of Oklahoma, Norman, Oklahoma 73019
[22]Purdue University, West Lafayette, Indiana 47907
[23]University of Rochester, Rochester, New York 14627
[24]Stanford Linear Accelerator Center, Stanford University, Stanford, California 94309
[25]Southern Methodist University, Dallas, Texas 75275

The semileptonic decays of the B meson play important roles in heavy quark physics. They provide our best information on the CKM matrix element V_{cb} and V_{ub} [1] and reveal the dynamics of heavy quark decay in their form factors. Heavy Quark Effective Theory (HQET) [2] provides a framework for calculating the form factors for $b \to c\ell\bar{\nu}$ decays and suggests a reliable method for extracting V_{cb} by predicting that QCD effects are small at the kinematic point where the final state meson is at rest relative to the initial meson (zero-recoil). We can measure the form factors and $|V_{cb}|$ using both $B \to D^*\ell\bar{\nu}$ and $B \to D\ell\bar{\nu}$ decays, though most studies have used $B \to D^*\ell\bar{\nu}$ [3] because its differential branching fraction near the zero-recoil region is large and the QCD effects have been calculated to the highest accuracy. There has been one precision study of the sister mode $B \to D\ell\bar{\nu}$ [4]. Here we present a new, more precise measurement using a different analysis method.

We select D's and leptons from the decay of a single B. This sample contains $B \to D\ell\bar{\nu}$, $B \to D^*\ell\bar{\nu}$, $B \to D^{**}\ell\bar{\nu}$, and $B \to D^{(*)}\pi\ell\bar{\nu}$. We separate $B \to D\ell\bar{\nu}$ from the other decays using a distribution that is sensitive to the invariant mass of the particle or particles recoiling against the $D - \ell$ pair. We also fit the differential decay rate as a function of the HQET variable $w = (M_B^2 + M_D^2 - q^2)/(2M_BM_D)$, where q^2 is the invariant mass-squared of the W^*, to study form factor and obtain the differential decay rate at zero-recoil.

The data used in this analysis were accumulated by the CLEO detector [5] at the Cornell Electron Storage Ring (CESR). The data consist of 3.1 fb^{-1} taken at the $\Upsilon(4S)$ resonance, corresponding to 3.3 million $B\bar{B}$ events. We also use 1.6 fb^{-1} of data taken 60 MeV below the $\Upsilon(4S)$ peak to study the background arising from the continuum $e^+e^- \to q\bar{q}$. The CLEO detector measures the trajectories of charged particles in a drift chamber system inside a 1.5T superconducting solenoid. We distinguish π's from K's based on their specific ionization (dE/dx) in the main drift chamber and their time-of-flight (TOF) to scintillator counters surrounding the drift chamber. A CsI electromagnetic calorimeter is used in electron identification. Muons register hits in counters embedded in steel surrounding the magnet.

In this analysis, we select hadronic events having at least 5 charged tracks and, to suppress non-$B\bar{B}$ events, the ratio of Fox-Wolfram moments [6] $H_2/H_0 < 0.45$. We reconstruct D^0 and D^+ candidates in the decay modes $D^0 \to K^-\pi^+$ and $D^+ \to K^-\pi^+\pi^+$, respectively. We distinguish K's from π's based on a χ^2 probability (P_K and P_π) that combines dE/dx and TOF information. We require that each daughter track satisfies $P_i > 0.01$ and $P_i/(P_K+P_\pi) > 0.3$, where i is π or K, whichever is appropriate. The candidate mass must be within 1.835 GeV $< m_{K\pi} <$ 1.893 GeV for D^0 and 1.846 GeV $< m_{K\pi\pi} <$ 1.890 GeV for D^+. To suppress D's produced in $e^+e^- \to c\bar{c}$ events, we require $|\vec{p}_D| < 2.5$ GeV$/c$.

Electrons are identified using dE/dx, the ratio of the energy deposited in the CsI calorimeter to the momentum measured in the drift chamber and the shape of the electromagnetic shower in the CsI. They are required to have momentum between 0.8 GeV$/c$ and 2.4 GeV$/c$. Muon identification requires penetration through at least 5 interaction lengths of material. This requirement effectively places a lower bound on the muon momentum of about 1.4 GeV$/c$. We require that the lepton have the same charge as the K from the decay of the D meson. Since the B is nearly at rest, the D meson and the lepton are in opposite hemispheres for more than 90% of $B \to D\ell\bar{\nu}$ decays; we demand that this be so.

For events satisfying these criteria, we compute $\theta_{B-D\ell}$, the angle between the $D\ell$ momentum $\vec{p}_{D\ell} = \vec{p}_D + \vec{p}_\ell$ and the B momentum $\vec{p}_B$, where we assume that the decay is $B \to D\ell\bar{\nu}$ and the only missing particle is the massless neutrino. That is

TABLE I. Event Yields and backgrounds. Uncertainties are statistical only.

	$D^0\ell$	$D^+\ell$
Total Yield	6249 ± 79	8958 ± 95
Random $K\pi(\pi)$ Combinations	2208 ± 33	5868 ± 46
Uncorrelated	333 ± 37	327 ± 43
Continuum	430 ± 43	374 ± 57
Correlated	70 ± 10	67 ± 14
Fake Lepton	50 ± 14	23 ± 20
Background-subtracted Yield	3158 ± 104	2299 ± 130

$$\cos\theta_{B-D\ell} = \frac{2E_B E_{D\ell} - M_B^2 - M_{D\ell}^2}{2|\vec{p}_B||\vec{p}_{D\ell}|}. \tag{1}$$

This quantity lies between -1.0 and 1.0 for $B \to D\ell\bar{\nu}$ decays. When final-state particles are missing in addition to the $\bar{\nu}$, as is the case for the other B semileptonic decay modes, $\cos\theta_{B-D\ell}$ decreases. We use the distribution of $\cos\theta_{B-D\ell}$ to separate $B \to D\ell\bar{\nu}$ events from the other B semileptonic decay modes after subtracting backgrounds.

Backgrounds come from several sources: random $K\pi(\pi)$ combinations, D mesons matched with a lepton from the other B decay (uncorrelated), D mesons combined with a lepton that is a granddaughter of the same B (correlated), fake leptons, and $e^+e^- \to q\bar{q}$ continuum events. Events in the mass regions above and below the D peak (sideband) are utilized to estimate the random combination contribution. A study using Monte Carlo simulated B decays shows that this method subtracts the right amount of background within small errors and that the $\cos\theta_{B-D\ell}$ distribution of the event's sidebands reproduces that of the background events in signal region. In uncorrelated background events, the directions of the D and ℓ are not correlated since the two parent B's are almost at rest. The number of events in which the uncorrelated D and ℓ are in the same hemisphere is therefore nearly the same as the number in which the D and ℓ are in opposite hemispheres. To construct the $\cos\theta_{B-D\ell}$ distribution of this source of background, we reverse the lepton direction of each same hemisphere event. The distribution in $\cos\theta_{B-D\ell}$ from continuum background is obtained using events collected off-resonance. The correlated background, which is small, arises from modes such as $B \to D_s D$ followed by $D_s \to X\ell\bar{\nu}$ and $B \to DX\tau\bar{\nu}$ followed by $\tau \to \ell\bar{\nu}\nu$. We estimate these contributions using a Monte Carlo simulation. Fake lepton background is estimated by repeating the analysis using non-leptonic tracks in place of lepton tracks and then scaling the yield by the momentum-dependent electron and muon misidentification probabilities. Table I summarizes the data yield and the number of events from various backgrounds.

After subtracting the backgrounds, we are left with $B \to D^0X\ell\bar{\nu}$ and $B \to D^+X\ell\bar{\nu}$ decays, where X stands for zero or more pions. We fit the $\cos\theta_{B-D\ell}$ distributions of these samples for the normalizations of $D\ell\bar{\nu}$, $D^*\ell\bar{\nu}$ and the sum of $D^{**}\ell\bar{\nu}$ and $D^{(*)}\pi\ell\bar{\nu}$, applying the isospin symmetry constraint that the ratio of vector to pseudo-scalar rates should be the same for charged and neutral B-meson decays. We take the $\cos\theta_{B-D\ell}$ distribution expected for each of those modes from a Monte Carlo simulation. We model $B \to D^*\ell\bar{\nu}$ decays using the form factors measured by CLEO [3]. We use ISGW2 to model D^{**} charm mesons

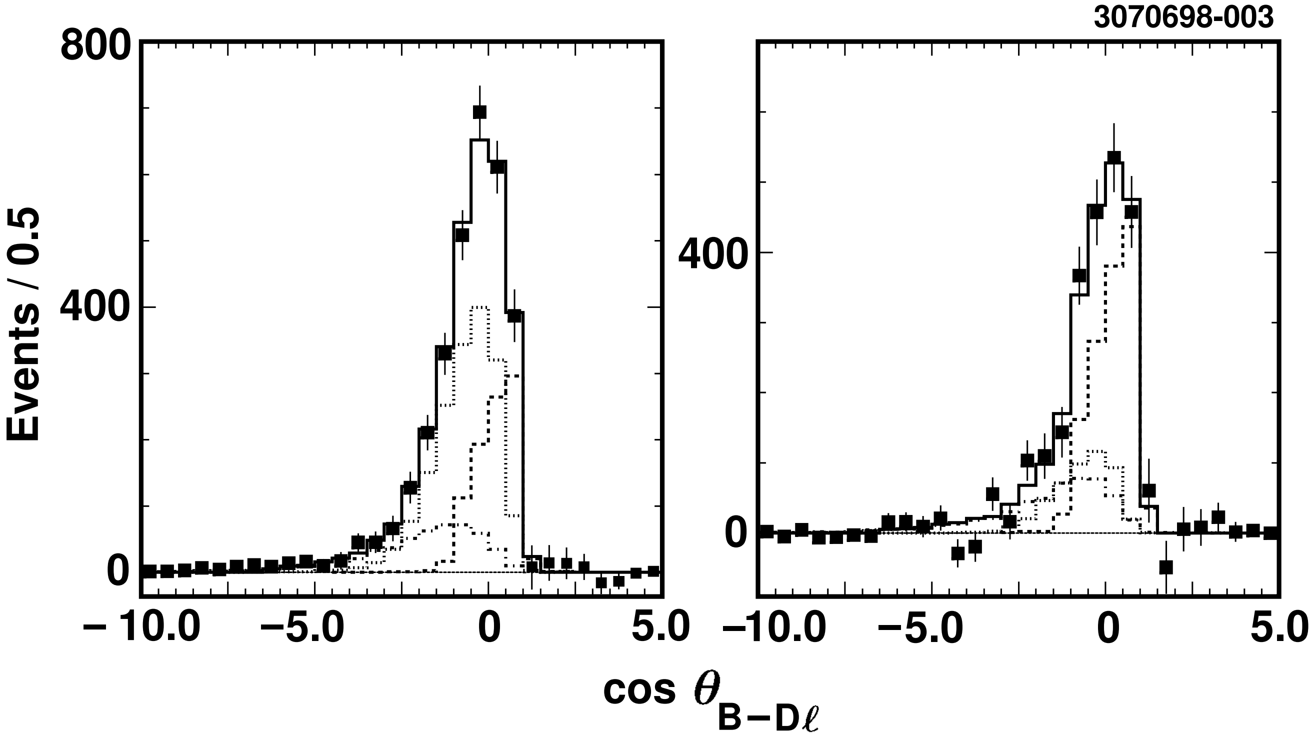

FIG. 1. The $\cos\theta_{B-D\ell}$ distribution for $B^- \to D^0 X\ell\bar{\nu}$ (left) and $\bar{B}^0 \to D^+ X\ell\bar{\nu}$ (right). The data (solid squares) are overlaid with simulated $B \to D\ell\bar{\nu}$ decays (short dashed histogram), $B \to D^*\ell\bar{\nu}$ decays (dotted histogram), $B \to D^{**}\ell\bar{\nu} + D^{(*)}\pi\ell\bar{\nu}$ decays (long dash-dotted histogram), and their total (solid histogram). The normalizations of the simulated samples are provided by the fit.

with radial and angular excitations and the results of Goity and Roberts [8] to simulate non-resonant $D^{(*)}\pi$ states. For all modes, we use a simulation of the detector based on GEANT [9]. Figure 1 shows the result of a fit using ISGW2 to model $B \to D\ell\bar{\nu}$ decays as an example.

To extract our results, we use the differential decay width $d\Gamma/dw$ in eight w intervals. The differential decay width of $B \to D\ell\bar{\nu}$ [11] is given by

$$\frac{d\Gamma}{dw} = \frac{G_F^2|V_{cb}|^2}{48\pi^3}(m_B + m_D)^2 m_D^3 (w^2-1)^{3/2} F_D(w)^2, \tag{2}$$

where $F_D(w)$ is the form factor. We obtain the $D\ell\bar{\nu}$ yield in each of ten equal intervals in $\tilde{w}$ by fitting $\cos\theta_{B-D\ell}$ distribution, where $\tilde{w}$ is the reconstructed value of w, and is smeared due to the motion of the B and detector resolution. An efficiency matrix (ϵ_{ij}) accounts for this smearing of w as well as for the reconstruction efficiency. Each ϵ_{ij} is the fraction of events generated in the jth w bin that is reconstructed in the ith $\tilde{w}$ bin. We then do a χ^2 fit to these yields in the intervals with $\tilde{w} > 1.12$ to extract parameters describing the form factor and the intercept at $w = 1$, $|V_{cb}|F_D(1)$. The χ^2 function for $B^- \to D^0\ell\bar{\nu}$ is expressed as

$$\chi^2_{B^-\to D^0\ell\bar{\nu}} = \sum_{i=3}^{10} \frac{[N_i^{obs} - \sum_{j=1}^{10}\epsilon_{ij}N_j]^2}{\sigma^2_{N_i^{obs}} + \sum_{j=1}^{10}\sigma^2_{\epsilon_{ij}}N_j^2}, \tag{3}$$

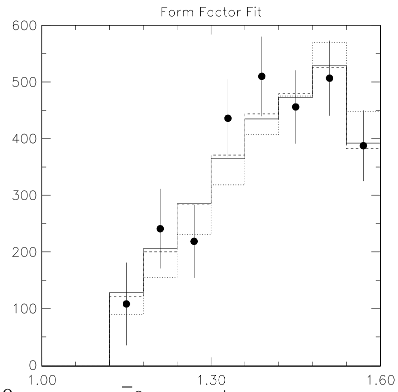

FIG. 2. The sum of $B^- \to D^0\ell\bar{\nu}$ and $\bar{B}^0 \to D^+\ell\bar{\nu}$ yields as a function of $\tilde{w}$, for the data (solid squares) and as predicted using the form factor from a linear expansion in w (dashed histogram), from the ISGW2 model (dotted histogram) and Boyd *et al.* (solid histogram).

where N_i^{obs} is the yield in the ith $\tilde{w}$ bin and N_j is the predicted differential decay rate integrated over the jth w bin calculated using the fit parameters and the measured B lifetimes $\tau_{\bar{B}^0}$ and τ_{B^-} [10]. The small statistical uncertainty in the efficiency matrix is represented by $\sigma^2_{\epsilon_{ij}}$. We form $\chi^2_{\bar{B}^0\to D^+\ell\bar{\nu}}$ using the same structure.

We first parametrize the form factor as $F_D(w) = F_D(1)\big(1 - \rho^2_D(w-1) + c_D(w-1)^2\big)$. A fit assuming a linear form factor ($c_D = 0$), shown in Figure 2, gives

$$\rho^2_D = 0.81 \pm 0.14 \tag{4}$$
$$|V_{cb}|F_D(1) = (4.31 \pm 0.42) \times 10^{-2}, \tag{5}$$

where the uncertainties are statistical only. The correlation coefficient between these parameters is 0.950. The χ^2 is 8.0 for 14 degrees of freedom.

We next allow the curvature c_D of the form factor to vary in the fit. The results are:

$$\rho^2_D = 0.50^{+1.25}_{-3.02} \tag{6}$$
$$c_D = -0.46^{+1.80}_{-4.28} \tag{7}$$
$$|V_{cb}|F_D(1) = (4.07^{+1.52}_{-1.64}) \times 10^{-2}. \tag{8}$$

The χ^2 of the fit is 7.0 for 13 degrees of freedom. We find a correlation between ρ^2_D and c_D of 0.996, as shown in Figure 3, that arises because our data are most precise at large values of w due to the large number of signal decays at large w arising from the p^3_D factor in the expression for $d\Gamma/dw$ and the large background from $D^*\ell\bar{\nu}$, $D^{**}\ell\bar{\nu}$, and $D^{(*)}\pi\ell\bar{\nu}$ at low values of w. The correlation is described by $c_D = 1.43(\rho^2_D - (\rho^2_D)_0)$ where $(\rho^2_D)_0 = 0.81 \pm 0.14$. In the same way, we find $|V_{cb}|F_D(1) = |V_{cb}|(F_D(1))_0 + 1.5(\rho^2_D - (\rho^2_D)_0)$, where $|V_{cb}|(F_D(1))_0 = (4.43 \pm 0.42) \times 10^{-2}$.

We also test the form factor using the ISGW2 model. The form factor parameterization [7] gives only one free parameter. The fit result is:

$$|V_{cb}|F(1) = (3.57 \pm 0.11) \times 10^{-2} \tag{9}$$

The χ^2 of the fit is 12.2 for 15 degrees of freedom. The increase in χ^2 arises because ISGW2 gives a harder spectrum in w than do our fits to the data, as shown in Figure 2.

Dispersion relations coupled with analyticity can constrain the form factor. Boyd *et al.* [14] expand the form factor in the variable $z = (\sqrt{w+1} - \sqrt{2N})/(\sqrt{w+1} + \sqrt{2N})$ where $N \approx 1.1$. Unlike an expansion in $w - 1$, for which even the third order term can be large, Boyd *et al*. find that the quadratic and higher order term in the z expansions shift the form factor by less than 2.6% at all values of w. Using this form and fitting for the linear coefficient a_1, we find

$$a_1 = -0.049 \pm 0.023 \tag{10}$$

$$|V_{cb}| F_D(1) = (4.78 \pm 0.57) \times 10^{-2} \tag{11}$$

with a χ^2 of 8.4 for 14 degrees of freedom and a correlation coefficient of -0.966. A change of variables relates the coefficients of the expansion in z to ρ_D^2 and c_D; however, their values are sensitive to the second order coefficient a_2, which our data do not constrain. Caprini *et al*. [15], find that a_2 is small. Assuming $a_2 = 0$, our value of a_1 gives $\rho_D^2 = 1.32 \pm 0.21$ and $c_D = 0.16 \pm 0.47$.

To obtain the $B \to D\ell\bar{\nu}$ decay rate, we use the form factor parameters provided by the fits and integrate $d\Gamma/dw$ over w. To eliminate the assumption that the B^+B^- and $B^0\bar{B}^0$ production fractions (f_{+-} and f_{00}) are equal, we note that if we separately determine $\Gamma^{\frac{1}{2}}(B^- \to D^0\ell\bar{\nu})$ and $\Gamma^{\frac{1}{2}}(\bar{B}^0 \to D^+\ell\bar{\nu})$, assuming $f_{+-} = f_{00} = 1/2$, then these can be related to the actual $\Gamma(B \to D\ell\bar{\nu})$ width by

$$\Gamma^{\frac{1}{2}}(B^- \to D^0\ell\bar{\nu}) = 2f_{+-}\Gamma(B \to D\ell\bar{\nu}) \tag{12}$$

$$\Gamma^{\frac{1}{2}}(\bar{B}^0 \to D^+\ell\bar{\nu}) = 2f_{00}\Gamma(B \to D\ell\bar{\nu}). \tag{13}$$

Adding these expressions and using $f_{+-} + f_{00} = 1$ gives

$$\Gamma(B \to D\ell\bar{\nu}) = \frac{1}{2}(\Gamma^{\frac{1}{2}}(B^- \to D^0\ell\bar{\nu}) + \Gamma^{\frac{1}{2}}(\bar{B}^0 \to D^+\ell\bar{\nu})). \tag{14}$$

This expression allows us to extract $\Gamma(B \to D\ell\bar{\nu})$ from our data assuming only that B^+B^- and $B^0\bar{B}^0$ together saturate $\Upsilon(4S)$ decays. A fit using Boyd *et al.* [14] gives

$$a_1 = -0.051 \pm 0.023 \tag{15}$$

$$\Gamma^{\frac{1}{2}}(B^- \to D^0\ell\bar{\nu}) = (15.2 \pm 1.9) ns^{-1} \tag{16}$$

$$\Gamma^{\frac{1}{2}}(\bar{B}^0 \to D^+\ell\bar{\nu}) = (13.6 \pm 1.2) ns^{-1}. \tag{17}$$

Combining these according to Equation 14, taking into account correlations arising because of the shared value of a_1, and using B lifetimes, we find

$$\Gamma(B \to D\ell\bar{\nu}) = (14.4 \pm 1.2) ns^{-1} \tag{18}$$

$$\mathcal{B}(B^- \to D^0\ell\bar{\nu}) = (2.33 \pm 0.19)\% \tag{19}$$

$$\mathcal{B}(\bar{B}^0 \to D^+\ell\bar{\nu}) = (2.25 \pm 0.19)\% \tag{20}$$

where the errors are statistical and are completely correlated. The other parametrizations of the form factor give the same value for the decay rate within 2%.

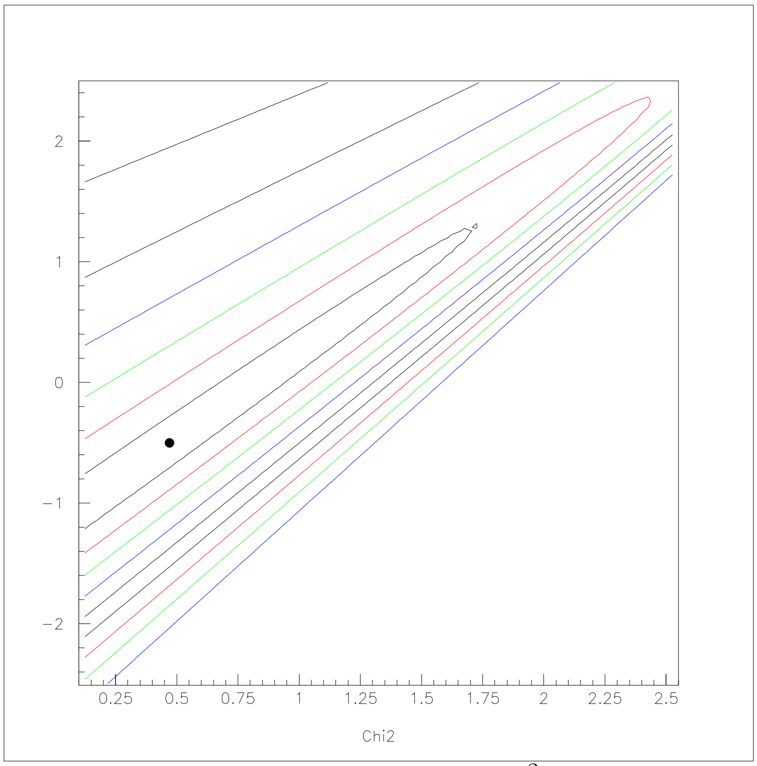

FIG. 3. χ^2 contours in the plane of c_D (y axis) versus ρ_D^2 (x axis). The dot is at our best fit and the contours are at 1σ, 2σ ... 9σ.

The systematic uncertainties are given in Table II. The uncertainties in the B meson momentum and mass dominate, because they affect the mean and the width of the $\cos\theta_{B-D\ell}$ distributions. Using fully reconstructed B decays we find an (8 ± 6) MeV B momentum difference between data and our Monte Carlo simulated events. Correcting for this shifts our results by the fractions of 5.4% for $B^- \to D^0\ell\bar{\nu}$, 1.4% for $\bar{B}^0 \to D^+\ell\bar{\nu}$, 0.9% for ρ_D^2 and 0.1% for $|V_{cb}|F_D(1)$. These changes have been applied to the results quoted above. The corresponding systematic uncertainties are 4.1%, 0.9%, 0.1%, and 0.5% respectively. The 1.8 MeV [12] uncertainty in the world average B mass generates relative uncertainties of 2.3% for $\mathcal{B}(B^- \to D^0\ell\bar{\nu})$, 1.0% for $\mathcal{B}(\bar{B}^0 \to D^+\ell\bar{\nu})$, 6.7% for ρ_D^2, and 3.7% for $|V_{cb}|F_D(1)$.

The other large systematic error is from uncertainty in the $\cos\theta_{B-D\ell}$ distribution of $B \to D^{**}\ell\bar{\nu}$ and $B \to D^{(*)}\pi\ell\bar{\nu}$ backgrounds. This distribution depends mainly on the number of final state pions that are not reconstructed. We therefore separate it into two components, one in which the final state D is accompanied by one π and the other in which it is accompanied by two. We vary their relative proportions from 1:4 to 2:3 [13] to evaluate the systematic uncertainty.

The $B \to D^*\ell\bar{\nu}$ form factors affect their distribution in $\cos\theta_{B-D\ell}$ and therefore influence the extracted $B \to D\ell\bar{\nu}$ yield. We vary the form factors within the uncertainties of the CLEO measurement [3], taking into account the correlations among the form factor parameters (R_1, R_2 and ρ^2).

The uncertainty in the $B \to D\ell\bar{\nu}$ form factor is largely accounted for in the fit. A small additional error arise from the systematic uncertainty in the form factor slope.

The remaining systematic uncertainties are small. We study correlated background by

TABLE II. The fractional systematic uncertainties assigned to $\mathcal{B}(B \to D\ell\bar{\nu})$ and form factor parameters.

Source	$B^- \to D^0\ell\bar{\nu}$	$\bar{B}^0 \to D^+\ell\bar{\nu}$	$\Gamma(B \to D\ell\bar{\nu})$	$\lvert V_{cb}\rvert F(1)$	ρ_D^2
Track-finding	0.03	0.04	0.04	0.02	-
Lepton ID	0.02	0.02	0.02	0.01	-
K and π ID	0.02	0.02	0.02	0.01	0.02
Random $K\pi(\pi)$ Background	0.02	0.01	0.01	0.02	0.02
Uncorrelated Background	0.02	0.01	0.02	0.01	0.01
Correlated Background	0.01	0.01	0.01	0.03	0.06
Fake leptons	0.01	0.01	0.01	0.01	-
$\lvert\vec{P}_B\rvert$ and M_B	0.04	0.01	0.03	0.04	0.07
Luminosity	0.02	0.02	0.02	0.01	-
$D\ell\bar{\nu}$ Form Factor	0.03	0.03	0.03	0.02	-
$D^*\ell\bar{\nu}$ Form Factors	0.01	0.01	0.01	0.01	0.04
$D^{**}\ell\bar{\nu}$ Model	0.02	0.04	0.03	0.03	0.04
Total	0.08	0.08	0.08	0.07	0.11
D branching fractions	0.03	0.07	0.04	0.02	-
τ_B	0.04	0.04	0.04	0.02	-

varying the branching fractions of the contributing modes. We study the random combinatoric and uncorrelated backgrounds using a large sample of Monte Carlo simulated B decays.

Our final results are:

$$\mathcal{B}(B^- \to D^0\ell\bar{\nu}) = (2.33 \pm 0.19 \pm 0.19 \pm 0.14)\% \tag{21}$$

$$\mathcal{B}(\bar{B}^0 \to D^+\ell\bar{\nu}) = (2.25 \pm 0.19 \pm 0.18 \pm 0.13)\% \tag{22}$$

where the first uncertainty is statistical, the second is systematic, and the third arises from the uncertainties in τ_B and $\mathcal{B}(D^0 \to K^-\pi^+)$ and $\mathcal{B}(D^+ \to K^-\pi^+\pi^+)$. Since we derive both branching fractions from the decay width, the errors are completely correlated. Our branching fractions are consistent with the previous measurement but are somewhat more precise. For the form factor slope, our linear fit gives $\rho_D^2 = 0.81 \pm 0.14 \pm 0.09$. If instead we use an expansion in z, we find $a_1 = -0.049 \pm 0.023 \pm 0.017$. This corresponds to $\rho_D^2 = 1.32 \pm 0.21 \pm 0.15$ if we assume $a_2 = 0$. Our differential decay rate at zero-recoil is sensitive to assumptions about the shape of the form factor. Various authors have found $F_D(1) = 0.98 \pm 0.07$ [16], $F_D(1) = 1.03 \pm 0.07$ [7], and recently lattice calculations have given the preliminary value, $F_D(1) = 1.069 \pm 0.029$ [17]. Using $F_D(1) = 1$ and Equation 11, we find $|V_{cb}| = 0.048 \pm 0.006 \pm 0.003 \pm 0.001 \pm 0.005$, where the uncertainties appear in the same order as for the branching fractions, but the last also includes a theoretical uncertainty of ± 0.1 in $F_D(1)$. This value of $|V_{cb}|$ is consistent with the measurements using $B \to D^*\ell\bar{\nu}$ decays, though the uncertainty is larger.

We thank C. Glenn Boyd for useful discussion. We gratefully acknowledge the effort of the CESR staff in providing us with excellent luminosity and running conditions. This work was supported by the National Science Foundation, the U.S. Department of Energy, the Heisenberg Foundation, the Alexander von Humboldt Stiftung, Research Corporation, the Natural Sciences and Engineering Research Council of Canada, and the A.P. Sloan Foundation.

REFERENCES

[1] N. Cabibbo, Phys. Rev. Lett. **10**, 531 (1963). M. Kobayashi and T. Maskawa, Prog. Theor. Phys. **49**, 652 (1973).

[2] N. Isgur and M.B. Wise, Phys. Lett. B **232**, 113 (1989); N. Isgur and M.B. Wise, Phys. Lett. B **237**, 527 (1990); M. Neubert, Phys. Lett. B **264**, 455 (1991); M. Neubert, Phys. Rep. **245**, 259 (1994).

[3] B. Barish *et al.*, Phys. Rev. D **51**, 1014 (1995);J.E. Duboscq *et al.*, Phys. Rev. Lett. **76**, 3898 (1996).

[4] M.Athanas *et al.*, Phys. Rev. Lett. **79**, 2208 (1997).

[5] Y. Kubota *et al.*, Nucl. Instrum. Methods Phys. Res., Sect. A **320**, 66 (1992).

[6] G. Fox and S. Wolfram, Phys. Rev. Lett. **41**, 1581 (1978).

[7] D. Scora and N. Isgur, Phys. Rev. D **52**, 2783 (1995); N. Isgur *et al.*, Phys. Rev. D **39**, 799 (1989).

[8] J.L. Goity and W. Roberts, Phys. Rev. D **51**, 3459 (1995).

[9] Applications Software Group, Computing and Networks Division, CERN, "GEANT, Detector Description and Simulation Tool", CERN Program Library Long Writeup Q123.

[10] $\tau_{B^-} = (1.62 \pm 0.06)$ps and $\tau_{\bar{B}^0} = (1.56 \pm 0.06)$ps, from Particle Data Group, Phys. Rev. D **54**, 477 (1996).

[11] J.D. Richman and P.R. Burchat, Rev. Mod. Phys. **67**, 893 (1995).

[12] Particle Data Group, Phys. Rev. D **54**, 477 (1996) .

[13] D. Buskulic *et al*, ALEPH Collaboration, Z. Phys. **C73**, 601 (1997)

[14] C. G. Boyd, B. Grinstein and R. F. Lebed, Phys. Rev. D **56**, 6895(1997). The dispersion relations provide constraint $f_+(w)P(w)\phi(w) = \sum a_n z^n$ where $\sum |a_n|^2 < 1$ and $P(w)$ and $\phi(w)$ are given in the reference and $f_+(w) = (1+r)/2\sqrt{r}F_D(w)$ with $r = m_D/m_B$.

[15] I. Caprini, L. Lellouch and M. Neubert, CERN-TH/97-91, hep-ph/9712417.

[16] I. Caprini and M. Neubert, Phys. Lett. B **380**, 376 (1996).

[17] Aida El-Khadra, Physics in Collisions Conference, 1998